

The Numerical Performance of Wavelets and Reproducing Kernels for PDE's

Mark A. Christon, David W. Roach, and Thomas E. Voth
Sandia National Laboratories
M/S 0819, P.O. Box 5800
Albuquerque, New Mexico 87185-0819

Summary

The results presented here constitute a brief summary of an on-going multi-year effort to investigate hierarchical/wavelet bases for solving PDE's and establish a rigorous foundation for these methods. A new, hierarchical, wavelet-Galerkin solution strategy based upon the Donovan-Geronimo-Hardin-Massopust (DGHM) compactly-supported multi-wavelet is presented for elliptic partial differential equations. This multi-scale wavelet-Galerkin method uses a wavelet transform to yield nearly mesh independent condition numbers for elliptic problems as opposed to the multi-scaling functions that yield condition numbers which increase as the square of the mesh size. In addition, the results of von Neumann analyses for the DGHM multi-wavelet element and the Reproducing Kernel Particle Method (RKPM) are presented for model hyperbolic partial differential equations. RKPM exhibits excellent dispersion characteristics using a consistent mass matrix with the proper choice of refinement parameter and mass matrix formulation. In comparison, the wavelet-Galerkin formulation using the DGHM element delivers a frequency response comparable to a Bubnov-Galerkin formulation with a quadratic element.

Introduction

Wavelet bases promise the capability to compute multi-scale solutions to partial differential equations with potentially higher convergence rates than conventional finite difference and finite element methods, and their built-in adaptive nature offers the possibility of "automatic" adaptivity. Similarly, the Reproducing Kernel Particle Method (RKPM) has many attractive properties that make it ideal for treating a broad class of physical problems. For example, RKPM may be implemented in a "mesh-full" or a "mesh-free" manner and provides the ability to selectively tune the method, via the selection of the refinement parameter and window function, in order to achieve the requisite numerical performance. RKPM also provides a framework for performing hierarchical computations making it an ideal candidate for simulating multi-scale problems. Despite the promise of wavelet bases and RKPM, the application of new numerical methods to physical problems involving wave propagation, advection and diffusion raises many questions about the overall numerical performance, computational complexity, and parallelism of these solution techniques.

Over the past year, five hierarchical/wavelet formulations have been investigated in order to evaluate their numerical performance in terms of convergence rate, dispersive behavior, and computational complexity. The solution methods considered include the wavelet-Galerkin [1], wavelet-collocation [5], and reproducing kernel [4] methods. Particular emphasis has been placed on solution methods that use bases with compact support, reproduce $\{1, x, y, xy, \dots\}$ in a consistent manner, accommodate a variety of boundary conditions, exhibit good dispersion characteristics, and provide a framework for hierarchical computations. Based upon the preliminary scoping efforts, the wavelet-Galerkin and reproducing kernel methods were selected for detailed study because these methods may be used as discrete frameworks with a variety of bases and have demonstrated application to realistic physical problems. In this summary, attention is focused on the dispersive nature of RKPM using cubic-spline window functions, and on the DGHM multi-wavelet element[2].

Formulation

This section presents a brief overview of the RKPM formulation, the DGHM multi-wavelet element, and a hierarchical solution algorithm based on the DGHM multi-wavelet. A detailed presentation of RKPM is beyond the scope of this work, and the reader is directed to the literature for details concerning the method [3,4].

The RKPM formulation begins with the definition of a kernel approximation to a function, u ,

$$u^R(x) = \int_{-\infty}^{+\infty} u(\xi)\varphi(x - \xi)d\xi, \tag{1}$$

where φ is a kernel function and u^R is the continuous approximation to u . In order to address a finite domain and discrete problems, numerical quadrature (e.g., trapezoidal integration) is used to evaluate Eq. (1) with a modified window function, $\bar{\varphi}$. The discrete kernel approximation is, in one-dimension,

$$u_h(x) = \sum_{i=1}^{Nnp} \bar{\varphi}(x - x_i)u(x_i)\Delta x_i, \tag{2}$$

where u_h is the discrete approximation to the function, u , and Nnp is the total number of nodes.

The modified, one-dimensional, window functions used in Eq. (2) are constructed with correction functions, $\beta_k(x)$, that vary within the domain, Ω [4]. The correction functions are designed so that the resulting discrete kernel approximation will consistently reproduce polynomials to the desired degree of approximation, i.e., consistently reproduce $\{1, x, x^2, \dots\}$. In two-dimensions, the window functions are obtained from a tensor product of the one-dimensional window functions with correction functions $\beta_k(x, y)$. From the modified window functions, shape functions in a finite element sense, may be obtained by considering Eq. (2) to be an expansion in terms of shape functions, i.e., $N_i(x) = \bar{\varphi}(x - x_i)\Delta x_i$.

In this work, a cubic spline is used as the window function, φ , with an optimal refinement parameter, $r = 1.14$, as established by Liu and Chen [3]. This refinement parameter is designed to minimize aliasing error in terms of an energy error. Note that if a linear “hat” function is used for the window function with $r = 1$, then the usual linear finite element shape functions are obtained.

With the RKPM formulation defined, attention is turned to the DGHM multi-wavelet element. Figure 1 shows the DGHM scaling and wavelet functions at the element level. Before proceeding with a description of the multi-scale Galerkin solution algorithm for elliptic partial differential equations, the mathematical framework is outlined. The problem under consideration is the solution to $-\epsilon \nabla^2 u + u = f$ with $\epsilon \geq 0$ and prescribed essential boundary conditions on Γ . In this context, let $V \subset \mathcal{H}$ be a subspace of a Hilbert space H , \mathcal{V}_h be a finite dimensional subspace of V , $a(u, v) = \int_{\Omega} u'v' + uv$ be a bounded symmetric coercive bilinear form on \mathcal{V} , and let $\mathcal{V}' (\cong \mathcal{V})$ denote the dual of \mathcal{V} .

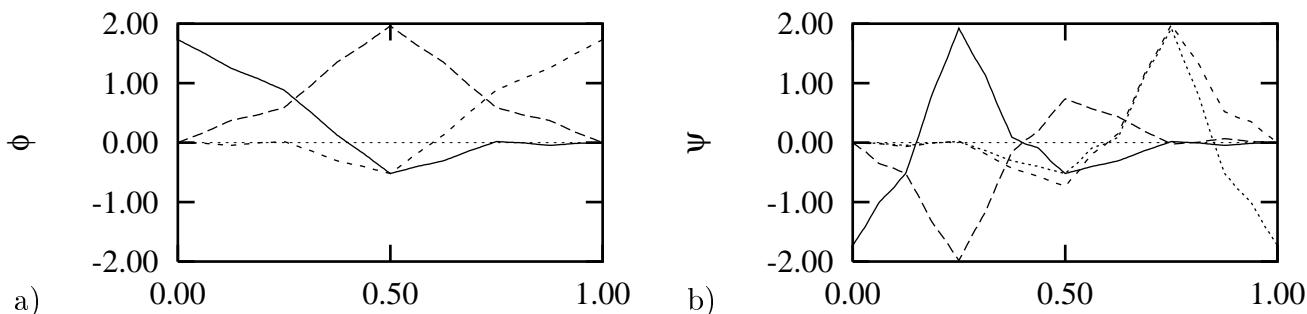


Figure 1: Donovan-Geronimo-Hardin-Massopust (DGHM) multi-wavelet element showing (a) the DGHM “shape” functions (ϕ), and (b) the element view of the multi-wavelet components (ψ).

In a Galerkin setting, given $f \in \mathcal{V}'$, the problem becomes one of finding $u_h \in \mathcal{V}_h$ such that $a(u_h, v) = (f, v)$, $\forall v \in \mathcal{V}_h$, where, $(\cdot, \cdot) = \int_{\Omega}(\cdot, \cdot)$. Throughout this section, a basis will be arranged as a column vector. Then u_h can be computed in terms of the scaling functions, Φ , as $u_h = c^T \Phi$. The coefficients, c , can be found by solving the linear system

$$\hat{K}^\Phi c = F(\Phi), \tag{3}$$

where $\hat{K}^\Phi = a(\Phi, \Phi)$ is an $Nnp \times Nnp$ matrix, i.e., the generalized stiffness, and $F(\Phi) = (f, \Phi)$ is the column vector $(F(\phi^1), \dots, F(\phi^N))^T$. For large Nnp , e.g., in three-dimensions, direct solution methods demand both large memory and cpu resources limiting the size of the linear system that may be solved. However, if the matrix, \hat{K}^Φ , can be preconditioned in an effective way, then the linear system can be efficiently solved using simple iterative techniques.

As an alternative to attempting to solve $\hat{K}^\Phi c = F$ by brute force, the wavelet basis Ψ , for \mathcal{V}_h is used to obtain a well-conditioned linear system. Given that Ψ is a multi-scale wavelet basis for \mathcal{V}_h , a multi-scale transform, W , may be constructed such that $\Psi = W^T \Phi$. The multi-scale transform is a nonsingular $Nnp \times Nnp$ matrix, and the transform, $\Psi = W^T \Phi$ can be implemented in an $O(Nnp)$ algorithm. Thus, in terms of the multi-wavelets, $u_h = d^T \Psi$ may also be found by solving

$$\hat{K}^\Psi d = F(\Psi). \tag{4}$$

Here, $\hat{K}^\Psi = a(\Psi, \Psi) = W^T \hat{K}^\Phi W$. Thus the linear system, Eq.(4), resulting from Eq.(3) via a change of basis can also be obtained by left and right preconditioning of \hat{K}^Φ with W . The solution of Eq. (3) using the multi-scale transformation W involves the following algorithm: 1) Approximate F^Φ , 2) Calculate $F^\Psi = W^T F^\Phi$, 3) Solve $W^T \hat{K}^\Phi W d = F^\Psi$, and 4) Evaluate $c = W d$. One important aspect of this algorithm is that it does not require the use of the wavelet decomposition matrix, W^{-1} .

With the RKPM and DGHM formulations outlined, attention is turned to the dispersion analysis. The application of discrete solution methods to wave propagation problems can yield results that are dispersive even when the physical problem is not dispersive. For this discussion, the two model problems under consideration are the first and second-order wave equations in Cartesian coordinates. The semi-discrete forms of the first and second-order wave equations are,

$$\mathbf{M}\dot{\mathbf{U}} + \mathbf{A}\mathbf{U} = 0, \quad \text{and} \quad \mathbf{M}\ddot{\mathbf{U}} + \mathbf{K}\mathbf{U} = 0, \tag{5}$$

where \mathbf{A} is the advection operator, and \mathbf{K} is the stiffness matrix. The generalized mass matrix is defined as $\mathbf{M} = \alpha \mathbf{M}^c + (1 - \alpha) \mathbf{M}^l$, where \mathbf{M}^c and \mathbf{M}^l are the consistent and row-sum-lumped mass matrices respectively, and $0 \leq \alpha \leq 1$. Details on the RKPM dispersion analysis may be found in [6].

In a Galerkin finite element setting, element level mass and stiffness operators for the one-dimensional DGHM element may be defined in terms of the scaling functions, Φ . The mass, M^e , and stiffness operator K^e associated with the second order wave equation are

$$M^e = \frac{l}{6} \begin{bmatrix} 1 & & \\ & 4 & \\ & & 1 \end{bmatrix}, \quad K^e = \frac{c^2}{21l} \begin{bmatrix} 85 & -128 & 43 \\ & 256 & -128 \\ \text{sym.} & & 85 \end{bmatrix}, \tag{6}$$

where c is the sonic velocity, $l = 2\Delta x$ is the element diameter, Δx is the node spacing, and a partition of unity scaling has been applied to the multi-wavelet scaling functions. Surprisingly, the element level mass matrix is identical to the row-sum lumped mass matrix for the quadratic finite element and is diagonal because the DGHM multi-wavelet scaling functions are orthogonal. Thus, the consistent mass for the DGHM element is diagonal. Because the multi-scale solution may be expressed in terms of the scaling functions alone, even when a multi-scale solution algorithm is used, this form of the mass and stiffness operator are sufficient to perform a von Neumann analysis.

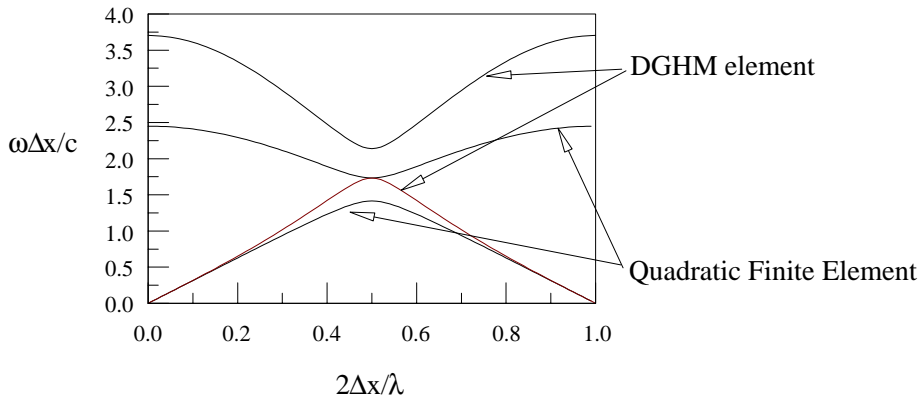


Figure 2: Non-dimensional circular frequency for the quadratic finite element and the DGHM multi-wavelet element.

Results

In order to evaluate the DGHM multi-wavelet element and the multi-scale transform algorithm the condition number associated with the generalized stiffness matrix was computed for both the multi-scaling functions and the multi-wavelets. The model problem considered is $-\epsilon u'' + u = f$ with $\epsilon \geq 0$, and $u(0) = u(L) = 0$. In the weak form, this problem becomes $M^\Phi U + K^\Phi U = F$.

Table 1 shows the condition numbers for both $\hat{K}^\Phi = [M^\Phi + K^\Phi]$ and $\hat{K}^\Psi = [M^\Psi + K^\Psi]$ after diagonal scaling for $0 \leq \epsilon \leq \infty$. Here, k indicates the scale with increasing k corresponding to increasing mesh resolution, i.e., $\Delta x = 2^{-(k+1)}$. As shown by the results, increasing the mesh resolution by a factor of 256 results in condition numbers that grow by 5 orders of magnitude for \hat{K}^Φ , while the condition numbers for \hat{K}^Ψ increase by only a factor of 10.

ϵ	0		1		10		100		10000		∞	
k	\hat{K}^Φ	\hat{K}^Ψ										
0	1	1	15	4	19	4	20	4	20	4	20	4
1	1	1	78	12	104	13	108	13	109	13	109	13
2	1	1	334	17	453	19	469	19	471	19	471	19
3	1	1	1355	24	1846	26	1915	26	1922	26	1923	26
4	1	1	5441	29	7418	31	7695	31	7727	31	7727	31
5	1	1	21785	33	29708	36	30818	36	30945	36	30947	36
6	1	1	87160	40	118866	40	123310	40	123819	40	123824	40
7	1	1	348662	44	475500	43	493276	43	495311	43	495332	43
8	1	1	1394668	47	1902035	46	1973143	46	1981282	46	1981365	46

Table 1: Condition numbers for the diagonally scaled \hat{K}^Φ and \hat{K}^Ψ operators for multiple mesh scales, $0 \leq k \leq 8$, and $0 \leq \epsilon \leq \infty$.

The non-dimensional frequency, $\omega\Delta x/c$, for the DGHM wavelet element is shown in Figure 2 with the frequency spectra for the quadratic finite element. The frequency response for each element admits two solutions, the so-called optical and acoustical branches. The gap between the branches of the frequency response is often referred to as a “stopping” band. The similarities between the spectra for the DGHM and quadratic elements suggests that the dispersive nature of the DGHM element will be similar to the behavior of the quadratic element, albeit with the inferior lumped mass matrix.

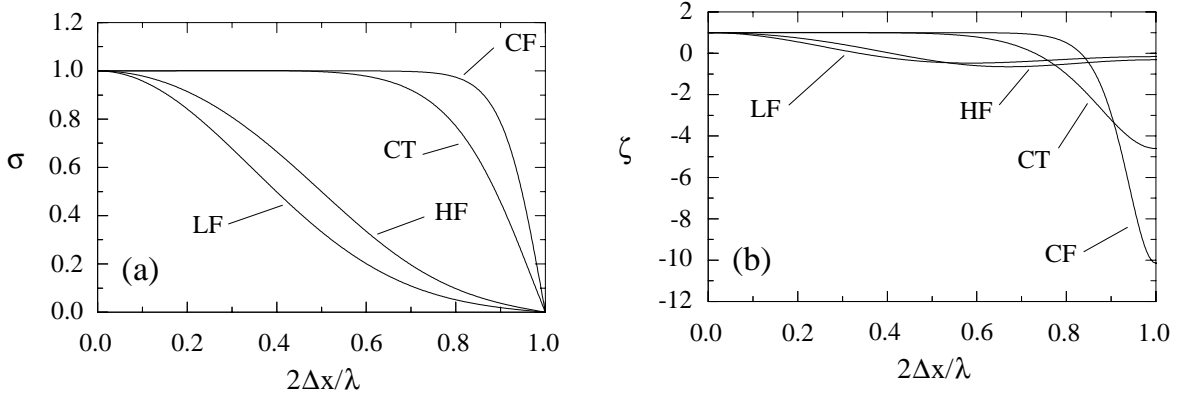


Figure 3: Non-dimensional phase (a) and group speed (b) for the one-dimensional, first-order wave equation. (CF: consistent mass, HF: higher-order mass, LF: lumped mass, CT: consistent mass - trapezoidal integration)

Attention is now turned to the results of a von Neumann analysis of the RKPM formulation for the first and second-order wave equation. The non-dimensional phase (σ) and group (ζ) speed for the semi-discrete, one-dimensional first-order and second-order wave equations are presented as functions of non-dimensional wave number, $k\Delta x/\pi = 2\Delta x/\lambda$, in Figures 3 and 4. For the first-order wave equation, the non-dimensional phase speed refers to the ratio between the discrete and continuum advective velocity, i.e., $\sigma = \bar{c}/c$ where \bar{c} is the discrete advective velocity. For the second-order wave equation, c is the sonic velocity. The non-dimensional group speed is defined as $\zeta = v_g/c$, where $v_g = \partial\omega/\partial k$, ω is the circular frequency, and k is the wave number. The results in Figures 3 and 4 are plotted for fully integrated, consistent (CF: $\alpha = 1$), lumped (LF: $\alpha = 0$), and higher-order (HF: $\alpha = 1/2$) mass matrix formulations along with with the consistent mass - trapezoidal integration (CT) formulation that uses nodes as quadrature points, eliminating the need for a background integration mesh.

For the first-order wave equation, the RKPM formulation introduces lagging phase errors over the discrete spectrum of wavelengths as shown in Figure 3. The consistent mass (CF) formulation performs the best and delivers significantly better phase and group speed relative to the lumped (LF) and “higher-order” (HF) mass matrix formulations. The consistent mass - trapezoidal integration (CT) formulation appears to offer a good trade-off between dispersive behavior and reduced computational cost.

Figure 4 shows the phase (a) and group (b) speed for the one-dimensional, second-order wave equation for the RKPM semi-discretization using the CF, CT, LF and HF formulations. Surprisingly, the trapezoidal mass formulation yields zero phase speed for $2\Delta x$ wavelengths, i.e., these wavelengths are stationary on the grid. Additionally, the CT formulation results in large, lagging group errors for wavelengths shorter than $3\Delta x$. In Figure 4(c), the fully integrated “bi-linear” RKPM formulation with a consistent mass matrix shows almost negligible phase errors with respect to the propagation direction, θ . Thus, the RKPM formulation yields nearly perfectly isotropic phase speed, i.e., there are no preferential propagation directions in two dimensions.

Conclusions

The DGHM multi-wavelet element in conjunction with the multi-scale wavelet transform is a promising new technology that offers the possibility of obtaining high-resolution results with nearly mesh-independent condition numbers for elliptic problems. The dispersive character of this new element is comparable to the quadratic finite element.

The results of the von Neumann analyses indicate that, for the formulations considered, the consistent mass RKPM formulations exhibit very good dispersion properties, e.g., phase errors less than

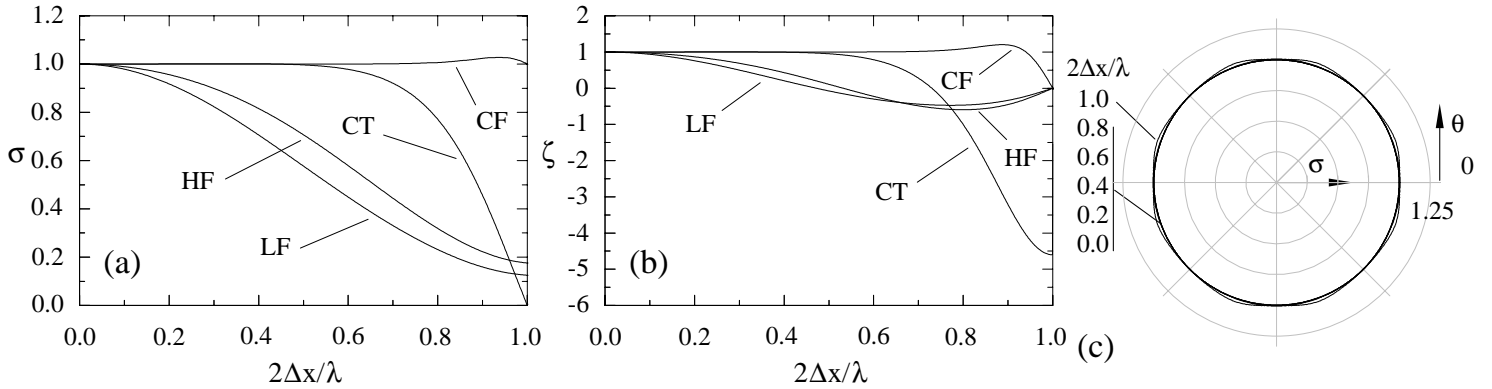


Figure 4: Phase (a) and group (b) speed for the one-dimensional, second-order wave equation, and phase speed (c) for a two-dimensional discretization with full integration and consistent mass. (CF: consistent mass, HF: higher-order mass, LF: lumped mass, CT: consistent mass - trapezoidal integration)

5% are obtained with only 3–4 nodes per wavelength. In addition, wave propagation with the consistent mass RKPM formulation in two-dimensions is nearly isotropic in terms of angular dependence of the phase speed and in terms of the amplitude of the phase errors. While the consistent mass matrix RKPM formulations perform quite well, the lumped and higher order mass formulations introduce severely lagging phase and group speeds. Finally, the consistent mass RKPM results indicate that minimal losses in phase and group speed error result when trapezoidal rather than full (Gauss) quadrature is used. The use of point-wise integration may significantly reduce computational cost by reducing the number of quadrature points needed, however, further testing with trapezoidal integration is required.

Acknowledgments

This work was supported by the U.S. DOE under Contract DE-AC04-94AL85000.

References

- [1] AMARTUNGA, K., AND WILLIAMS, J. R. (1994), Wavelet-Galerkin solutions for one-dimensional partial differential equations, International Journal for Numerical Methods in Engineering, Vol. 37, pp. 2703–2716.
- [2] KO, J., KURDILA, A. J., AND OSWALD, P. (1996), Multiscale Wavelet Methods for PDEs, ch. Scaling Function and Wavelet Preconditioners for Second Order Elliptic Problems, Academic Press, Inc., pp. 413–438.
- [3] LIU, W. K., AND CHEN, Y. (1995), Wavelet and multiple scale reproducing kernel methods. International Journal for Numerical Methods in Fluids, Vol. 21, pp. 901–931.
- [4] LIU, W. K., CHEN, Y., CHEN, J. S., BELYTSCHKO, T., PAN, C., CURAS, R. A., AND CHANG, C. T. (1996), Overview and applications of the reproducing kernel particle methods. Archives of Computational Methods in Engineering, Vol. 3, No. 1, pp. 3–80.
- [5] VASILYEV, O. V., AND PAOLUCCI, S. (1996) A dynamically adaptive multilevel wavelet collocation method for solving partial differential equations in a finite domain, Journal of Computational Physics, Vol. 125, pp. 498–512.
- [6] VOTH, T. E., AND CHRISTON, M. A. (1998) Results of von Neumann analyses for reproducing kernel semi-discretizations. In Fourth World Congress on Computational Mechanics (Buenos Aires, Argentina, June 1998).